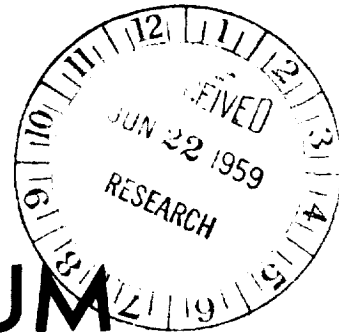


# NASA

# MEMORANDUM



STUDY OF THE OSCILLATORY MOTION OF MANNED VEHICLES  
ENTERING THE EARTH'S ATMOSPHERE

By Simon C. Sommer and Murray Tobak

Ames Research Center  
Moffett Field, Calif.

MAY 21 1959

CASE FILE  
COPY

PROPERTY OF NASA  
NOT TO BE REPRODUCED  
WITHOUT PERMISSION

NATIONAL AERONAUTICS AND  
SPACE ADMINISTRATION

WASHINGTON

April 1959

20  
x2



NATIONAL AERONAUTICS AND SPACE ADMINISTRATION

---

MEMORANDUM 3-2-59A

---

STUDY OF THE OSCILLATORY MOTION OF MANNED VEHICLES

ENTERING THE EARTH'S ATMOSPHERE

By Simon C. Sommer and Murray Tobak

SUMMARY

An analysis is made of the oscillatory motion of vehicles which traverse arbitrarily prescribed trajectories through the atmosphere. Expressions for the oscillatory motion are derived as continuous functions of the properties of the trajectory.

Results are applied to a study of the oscillatory behavior of re-entry vehicles which have decelerations that remain within limits of human tolerance. It is found that a deficiency of aerodynamic damping for such vehicles may have more serious consequences than it does for comparable ballistic missiles.

INTRODUCTION

Studies of the oscillatory behavior of missiles entering the atmosphere on ballistic trajectories (refs. 1 and 2) have revealed that the rapid increase in atmospheric density experienced by such vehicles is a potent factor in restraining the magnitude of their oscillations. In reference 2, for example, it is shown that even a vehicle that is dynamically unstable in the usual aerodynamic sense will undergo oscillations that are convergent over either all or the major portion of its path through the atmosphere. Generally, the conclusion has been that for ballistic missiles, dynamic instability is a potential source of difficulty only in their terminal phase of flight.

For the case of descending manned vehicles, the situation is not yet as clear. Since manned vehicles cannot be permitted to develop the very large decelerations experienced by ballistic missiles, means of reducing the decelerations must be introduced. A study of this problem by Chapman (ref. 3) has revealed that decelerations can be held within tolerable limits by the use of small amounts of lift and by the use of re-entry trajectories starting from very small initial flight-path angles. The question arises: What effect do these efforts to reduce deceleration have on the oscillatory motion?

A study of this question was undertaken by the authors, using as a starting point the results of an analysis of oscillatory motions over arbitrary trajectories presented by Tobak and Allen in reference 4. In the course of this study, it was discovered that a number of limitations and assumptions of the previous analysis could be eliminated, thus both widening its scope and simplifying its use. The purpose of the present paper is therefore twofold: first to re-examine the motion analysis of reference 4 to show how it can be extended, and second to apply the results to a study of the oscillatory behavior of a class of vehicles which have decelerations within the limits of human tolerance.

# SYMBOLS

A	reference area
$C_D$	drag coefficient, $\frac{\text{drag}}{qA}$
$C_L$	lift coefficient, $\frac{\text{lift}}{qA}$
$C_m$	pitching-moment coefficient, $\frac{\text{pitching moment}}{qAl}$
$C_{L_\alpha}$	rate of change of lift coefficient with angle of attack, $\left(\frac{\partial C_L}{\partial \alpha}\right)_{\alpha \rightarrow 0}$
$C_{m_\alpha}$	rate of change of pitching-moment coefficient with angle of attack, $\left(\frac{\partial C_m}{\partial \alpha}\right)_{\alpha \rightarrow 0}$
$C_{m_{\dot{\alpha}}}$	rate of change of moment coefficient with time rate of change of angle-of-attack parameter $\frac{\dot{\alpha}l}{V}$ , $\left(\frac{\partial C_m}{\partial \dot{\alpha}l/V}\right)_{\dot{\alpha} \rightarrow 0}$
$C_{m_q}$	rate of change of moment coefficient with pitching velocity parameter $\frac{\dot{\theta}l}{V}$ , $\left(\frac{\partial C_m}{\partial \dot{\theta}l/V}\right)_{\dot{\theta} \rightarrow 0}$
$C_{m_\delta}$	rate of change of moment coefficient with control deflection, $\left(\frac{\partial C_m}{\partial \delta}\right)_{\delta \rightarrow 0}$
D	drag

$\left. \begin{matrix} f_1(t) \\ f_2(t) \end{matrix} \right\}$	parameters defined by equation (6)
$g$	acceleration due to gravity
$I$	pitching moment of inertia about center of gravity
$J_0( )$	Bessel function of first kind of zero order
$K$	dynamic stability parameter (eq. (9))
$L$	lift
$l$	body length and reference length for moment coefficient evaluation
$M(s)$	parameter defined by equation (12)
$m$	vehicle mass
$\left. \begin{matrix} P_1(s) \\ P_2(s) \end{matrix} \right\}$	parameters defined by equation (9)
$q$	dynamic pressure, $\frac{1}{2} \rho V^2$
$r$	distance from center of earth to vehicle
$s$	distance measured along path of "static" trajectory (see text)
$t$	time
$u$	horizontal component of flight velocity (sketch (a))
$\bar{u}$	ratio of horizontal component of flight velocity to satellite velocity, $\frac{u}{\sqrt{gr}}$
$V$	flight velocity (sketch (a))
$\bar{V}$	ratio of flight velocity to satellite velocity, $\frac{V}{\sqrt{gr}}$
$v$	vertical component of flight velocity (sketch (a))
$W$	vehicle weight
$y$	altitude
$Y_0( )$	Bessel function of second kind of zero order
$X, Z$	axes fixed in space with origin at center of earth (sketch (a))

$\alpha$	angle of attack (sketch (a))
$\beta$	density parameter (eq. (32))
$\gamma$	flight-path angle (sketch (a))
$\delta$	control deflection angle
$\Theta$	angle of pitch measured from axis fixed in space (sketch (a))
$\theta$	angle of pitch measured from local horizontal (sketch (a))
$\rho$	air density
$\rho_0$	air density at sea level
$\sigma$	radius of gyration
$\phi$	angular displacement of vehicle from fixed space axis, $\theta - \Theta$ (sketch (a))
$(\dot{\phantom{a}})$	$\frac{d}{dt} ( \phantom{a} )$
$( \phantom{a} )'$	$\frac{d}{ds} ( \phantom{a} )$
$( \phantom{a} )_i$	initial value
$( \phantom{a} )_{\max}$	envelope curve of oscillatory motion
$( \phantom{a} )_o$	oscillatory variable
$( \phantom{a} )_s$	nonoscillatory variable

## ANALYSIS

Our purpose in the ensuing analysis is to show how a further improvement can be made in the expression developed in reference <sup>4</sup> for oscillatory motions over arbitrary trajectories. Specifically, we shall eliminate both the assumption of constant aerodynamic coefficients and the necessity of breaking the trajectory into straight-line segments.

### Equations of Motion

The equations of motion defining the vehicle's path and its oscillations about that path may be written as

$$\left. \begin{aligned} -m\dot{V} - C_D q A + mg \sin \gamma &= 0 \\ mV\dot{\gamma} + C_L q A + m\left(\frac{V^2}{r} - g\right) \cos \gamma &= 0 \\ I\ddot{\Theta} - qA\ell\Sigma C_m &= 0 \end{aligned} \right\} \quad (1)$$

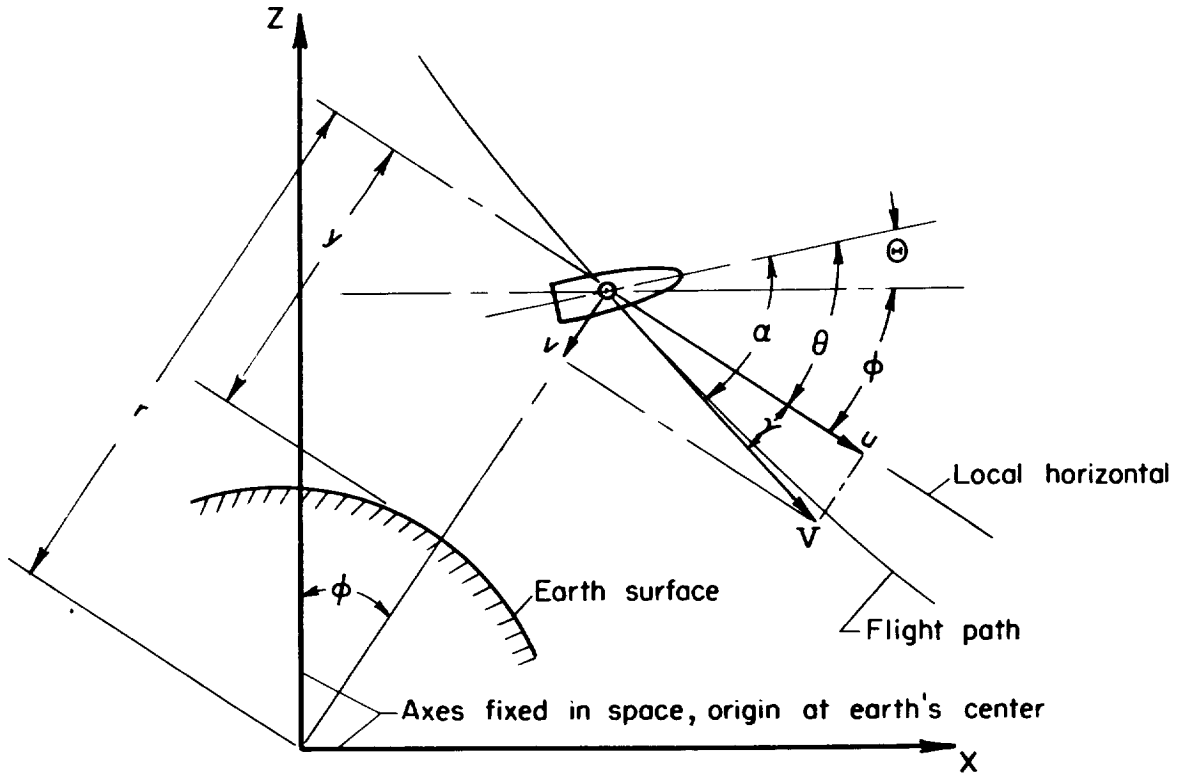
where

$$\Theta = \theta - \phi$$

$$C_L = C_{L_\alpha} \alpha$$

$$\Sigma C_m = C_{m_\alpha} \alpha + C_{m_\dot{\alpha}} \frac{\dot{\alpha}}{V} + C_{m_q} \frac{\dot{\Theta}}{V} + C_{m_\delta} \delta$$

The angles  $\alpha$ ,  $\gamma$ ,  $\theta$ ,  $\phi$ ,  $\Theta$  are defined in sketch (a). Note in both sketch (a) and equations (1) that we have taken this opportunity to correct an error that appears in the derivations of references 1 and 4; namely, the erroneous use therein of a moving rather than a fixed axis to define angular velocity ( $\dot{\Theta}$ ) and angular acceleration ( $\ddot{\Theta}$ ). This error does not affect the equations for oscillatory motion given in references 1 and 4, however, as will be seen.



Sketch (a)

Following the argument of reference 4, we now separate equations (1) into two sets of equations, one set  $(\gamma_s, \alpha_s, \Theta_s)$  defining the "static trajectory" of the center of gravity of the vehicle, the other  $(\gamma_o, \alpha_o, \Theta_o)$  defining the oscillatory motions of the vehicle about the static trajectory. Thus, under the restriction  $|\gamma_o/\gamma_s| \ll 1$ , we get for the static trajectory equations

$$\left. \begin{aligned} -m\dot{V} - C_D q A + mg \sin \gamma_s &= 0 \\ mV\dot{\gamma}_s + qAC_{L_\alpha}\alpha_s + m\left(\frac{V^2}{r} - g\right)\cos \gamma_s &= 0 \\ I\ddot{\Theta}_s - qAl\left(C_{m_\alpha}\alpha_s + C_{m_\alpha}\frac{\dot{\alpha}_s l}{V} + C_{m_q}\frac{\dot{\Theta}_s l}{V} + C_{m_\delta}\delta\right) &= 0 \end{aligned} \right\} \quad (2)$$

and for the oscillatory motion

$$\left. \begin{aligned} mV\dot{\gamma}_o + qAC_{L_\alpha}\alpha_o &= 0 \\ I\ddot{\Theta}_o - qAl\left(C_{m_\alpha}\alpha_o + C_{m_\alpha}\frac{\dot{\alpha}_o l}{V} + C_{m_q}\frac{\dot{\Theta}_o l}{V}\right) &= 0 \end{aligned} \right\} \quad (3)$$

We note, however, that  $\dot{\phi} = u/r$ , which is a nonoscillatory quantity. Hence, we may write

$$\left. \begin{aligned} \Theta_s &= \theta_s - \phi \\ \Theta_o &= \theta_o \end{aligned} \right\} \quad (4)$$

so that equations (3) for the oscillatory motion agree with equations (5) of reference 4. Again, use of the equality  $\theta_o = \alpha_o - \gamma_o$  permits the set of equations (3) to be combined into a single equation for the oscillatory angle of attack:

$$\ddot{\alpha}_o(t) + f_1(t)\dot{\alpha}_o(t) + f_2(t)\alpha_o(t) = 0 \quad (5)$$

with

$$\left. \begin{aligned} f_1(t) &= C_{L_\alpha} \frac{\rho VA}{2m} - \left(C_{m_q} + C_{m_\alpha}\right) \frac{\rho VA l^2}{2I} \\ f_2(t) &= -C_{m_\alpha} \frac{\rho V^2 A l}{2I} + \frac{d}{dt} \left( C_{L_\alpha} \frac{\rho VA}{2m} - \frac{C_{m_q} C_{L_\alpha}}{I m} \left( \frac{\rho VA l}{2} \right)^2 \right) \end{aligned} \right\} \quad (6)$$

Equations (2) through (6) retain with reference 4 the implicit assumption that the drag coefficient  $C_D$  is independent of angle of attack and pitching velocity. However, it need not be assumed that the aerodynamic coefficients in equations (2) through (6) are independent of Mach number.



## Oscillatory Motion

As in reference 4, henceforth the subscripts  $s$  and  $o$  will be omitted. It is to be understood that in referring to  $\alpha$  we mean the oscillatory angle of attack, whereas in referring to  $\gamma$  we mean the flight-path angle of the static trajectory. Now consider equation (5) for the oscillatory angle of attack and let the independent variable be distance traveled along the flight path,  $s$ . The use of  $s$  rather than  $y$  as independent variable has a twofold advantage: First,  $s$  is a single-valued function for any flight path and, second, the appearance of  $\sin \gamma$  is suppressed. With the substitutions

$$\left. \begin{aligned} \dot{\alpha}(t) &= \alpha'(s)V \\ \ddot{\alpha}(t) &= \alpha''(s)V^2 + \alpha'(s)V V'(s) \end{aligned} \right\} \quad (7)$$

in equation (5), we get for the oscillatory equation of motion

$$\alpha''(s) + \alpha'(s) \left[ \frac{V'(s)}{V} - P_1(s) \right] + P_2(s)\alpha(s) = 0 \quad (8)$$

with

$$\left. \begin{aligned} P_1(s) &= \frac{\rho}{2} \left( \frac{C_D A}{m} \right) K \\ K &= \frac{1}{C_D} \left[ -C_{L\alpha} + \left( \frac{l}{\sigma} \right)^2 (C_{mq} + C_{m\dot{\alpha}}) \right] \\ P_2(s) &= - \frac{\rho A l}{2I} C_{m\alpha} \end{aligned} \right\} \quad (9)$$

and where we have retained only the dominant term in  $P_2(s)$  (cf. appendix of ref. 4). The transformation

$$\alpha(s) = \bar{\alpha}(s) e^{-\frac{1}{2} \int \left[ \frac{V'(s)}{V(s)} - P_1(s) \right] ds} \quad (10)$$

then gives

$$\bar{\alpha}''(s) + M(s)\bar{\alpha}(s) = 0 \quad (11)$$

with

$$M(s) = P_2(s) - \frac{1}{2} \frac{d}{ds} \left[ \frac{V'(s)}{V} - P_1(s) \right] - \frac{1}{4} \left[ \frac{V'(s)}{V} - P_1(s) \right]^2 \quad (12)$$

Again as in reference 4, it is easy to show that  $M(s)$  is essentially  $P_2(s)$ .

Asymptotic solution for  $\bar{\alpha}(s)$ . - In reference 4, it was found that with the assumption of constant flight-path angle and constant  $C_{m\alpha}$  a solution to equation (11) could be written in terms of zero-order Bessel functions of the first and second kind. Experience with this solution has shown, however, that it approaches its asymptotic form very rapidly. This suggests that the asymptotic solution to equation (11) likewise should be of sufficient accuracy for most practical purposes. The advantage to seeking an asymptotic solution to equation (11) is of course that the above-mentioned assumptions need not be invoked. It is by this means, therefore, that the necessity of breaking the trajectory into a series of straight-line segments is eliminated.

To find the asymptotic solution to equation (11) we use a theorem given in its most general form by Wintner in reference 5. Wintner has shown that for large  $s$  any differential equation of the form (11) whose coefficient  $M(s)$  satisfies the conditions

$$M(s) > 0 \quad \text{for all } s \quad (13)$$

$$\int_0^{\infty} [M(s)]^{-1/2} \left| \frac{5}{4} \left( \frac{M'}{M} \right)^2 - \frac{M''}{M^2} \right| ds < \infty \quad (14)$$

will have a general solution which approaches asymptotically (as  $s \rightarrow \infty$ ) the form

$$\bar{\alpha}(s) = [M(s)]^{-1/4} [c_1 \cos \varphi(s) + c_2 \sin \varphi(s)] \quad (15)$$

where

$$\varphi(s) = \int \sqrt{M(s)} ds \quad (16)$$

Further, differentiation of the asymptotic representation (15) is allowed. Since, as has been mentioned,  $M(s)$  is essentially equal to  $P_2(s)$ , the condition  $M(s) > 0$  will be satisfied so long as the vehicle is statically stable ( $C_{m\alpha} < 0$ ) and its flight path remains within the measurable atmosphere ( $\rho > 0$ ). With  $M(s) > 0$  and twice differentiable, the condition (14) is readily satisfied for any flight path that terminates in a finite distance.

Hence, letting  $M(s)$  equal  $P_2(s)$  and combining equation (15) with (10), we have as an asymptotic solution for the oscillatory motion

$$\alpha(s) = \frac{1}{[V^2(s)P_2(s)]^{1/4}} e^{\frac{1}{2} \int P_1(s) ds} [c_1 \cos \varphi(s) + c_2 \sin \varphi(s)] \quad (17)$$

or

$$\alpha(s) = \frac{C_0}{[-C_{m_\alpha}(s)q(s)]^{1/4}} e^{\frac{1}{2} \int P_1(s) ds} \cos[\varphi(s) - \varphi_0] \quad (18)$$

with

$$\varphi(s) = \int \sqrt{P_2(s)} ds$$

Because of the mildness of the conditions affecting its generality, equation (18) is considered to be the central result of this analysis. However, it cannot be expected to apply accurately over the initial part of the motion. On the other hand, the Bessel function solution of reference 4 does apply to the initial motion, since over a sufficiently small interval  $\sin \gamma$  and  $C_{m_\alpha}$  will not change significantly. A simple artifice that combines these observations to give one expression that is applicable over the initial part of the motion and still has the correct asymptotic behavior is the following: Replace the asymptotic solution (15) by the Bessel function combination that has (15) as its asymptotic representation. Thus

$$\bar{\alpha}(s) = \left[ \frac{\varphi^2(s)}{M(s)} \right]^{1/4} \left\{ c_3 J_0[\varphi(s)] + c_4 Y_0[\varphi(s)] \right\} \quad (19)$$

and

$$\alpha(s) = \left[ \frac{\varphi^2(s)}{V^2(s)M(s)} \right]^{1/4} e^{\frac{1}{2} \int P_1(s) ds} \left\{ c_3 J_0[\varphi(s)] + c_4 Y_0[\varphi(s)] \right\} \quad (20)$$

where  $M(s) \approx P_2(s)$  and in  $\varphi(s)$  continuous variations in  $C_{m_\alpha}$  and  $\gamma$  are to be permitted. It can be verified that with  $C_{m_\alpha}$  and  $\sin \gamma$  constant,  $\varphi^2(s) = cM(s)$ , so that equation (20) then reduces to the form given in reference 4.

Further simplifications.— Equation (18) holds for any flight path that remains within the measurable atmosphere, and for arbitrary variations of the aerodynamic coefficients. When some of the coefficients can be considered constants, further simplifications are possible. As an example, let us assume that all coefficients are constants. The exponent in equation (18) then has the form

$$e^{\frac{1}{4} \left( \frac{C_D^A}{m} \right) K \int \rho(s) ds} \quad (21)$$

The integral can be evaluated by adopting the approximations introduced by Chapman in reference 3. Thus, consider the equation for balance of forces in the horizontal direction (cf. ref. 3):

$$m \left( \frac{du}{dt} + \frac{uv}{r} \right) + D \cos \gamma \left( 1 - \frac{L}{D} \tan \gamma \right) = 0 \quad (22)$$

Following Chapman, we neglect the terms  $uv/r$  and  $(L/D)\tan \gamma$  in equation (22) under the conditions that

$$\left. \begin{aligned} \frac{|uv/r|}{|du/dt|} &= \frac{|dr/r|}{|du/u|} \ll 1 \\ \left| \frac{L}{D} \tan \gamma \right| &\ll 1 \end{aligned} \right\} \quad (23)$$

The first of these conditions has been shown in reference 3 to be satisfied by any trajectory that has entered the atmosphere, since as soon as the drag becomes important in decelerating the motion the percentage change in  $u$  becomes large compared with the percentage change in distance from the planet center. The second condition is of course satisfied without approximation by nonlifting vehicles at any flight-path angle other than  $90^\circ$ . It should also be easily satisfied by lifting vehicles entering the atmosphere from satellite orbits for then  $\tan \gamma$  is generally very small. Equation (22) becomes

$$\frac{du}{dt} + \frac{1}{2} \left( \frac{C_D A}{m} \right) \rho \frac{u^2}{\cos \gamma} = 0 \quad (24)$$

and the transformation  $du/dt = (u/\cos \gamma)(du/ds)$  permits  $\rho(s)$  to be written as

$$\rho(s) = -2 \left( \frac{m}{C_D A} \right) \frac{1}{u} \frac{du}{ds} \quad (25)$$

Inserting equation (25) in (21) and integrating then gives for  $\alpha(s)$

$$\alpha(s) = \frac{C_1 u^{-K/2}}{[q(s)]^{1/4}} \cos[\varphi(s) - \varphi_0] \quad (26)$$

The envelope of the oscillation has the simple form

$$\alpha_{\max}(s) = \frac{C_1 u^{-K/2}}{[q(s)]^{1/4}} \quad (27)$$

### Convergence Criteria

General criterion.- Let us now return to the asymptotic solution for oscillatory motion (eq. (18)) and attempt to derive from it a criterion whose satisfaction ensures that the motion is convergent at any position  $s$  of the flight path. We use equation (18) rather than (26) since it turns out that a remarkably simple result can be obtained from equation (18) free of approximations either to the aerodynamic coefficients or to the flight path. Thus, noting that the envelope of the oscillation varies as

$$\alpha_{\max}(s) = \frac{C_0}{[-C_{m\alpha}(s)q(s)]^{1/4}} e^{\frac{1}{2} \int P_1(s) ds} \quad (28)$$

we have convergence at any position  $s$  provided  $\frac{d}{ds}(\alpha_{\max}) < 0$ . This is ensured if

$$\frac{P_1(s)}{2} - \frac{1}{4} \frac{q'(s)}{q(s)} - \frac{1}{4} \frac{C_{m\alpha}'(s)}{C_{m\alpha}(s)} < 0 \quad (29)$$

It will be noted that equation (29) has essentially the same form (for  $C_{m\alpha} = \text{const.}$ ) as the convergence criterion derived in reference 4. Equation (29) is the more convenient expression, however, in that it applies without change to any trajectory. With the use of  $y$  rather than  $s$  as independent variable the inequality of reference 4 must be reversed whenever  $\gamma$  changes sign.

The usefulness of the criterion (29) is enhanced if an expression in terms of primary quantities can be found for  $q'(s)/q(s)$ . Such an expression is obtainable from the first of the static trajectory equations (eq. (2)) in the following way. Converting the variable in equation (2) to altitude  $y$  by the transformation

$$\frac{dV}{dt} = \frac{dV}{dy} \frac{dy}{dt} = -(\sin \gamma) V \frac{dV}{dy} = -\frac{\sin \gamma}{2} \frac{d}{dy} (V^2) \quad (30)$$

we have

$$\frac{1}{2} \frac{d}{dy} (V^2) = \left( \frac{C_D A}{m} \right) \frac{q}{\sin \gamma} - g \quad (31)$$

Now introduce the well-known assumption that atmospheric density varies exponentially with altitude:

$$\rho = \rho_0 e^{-\beta y} \quad (32)$$

Use of equation (32) in the identity

$$\frac{1}{2} \frac{d}{dy} (v^2) = \frac{d}{dy} \left( \frac{q}{\rho} \right) \quad (33)$$

then gives

$$\frac{dq}{dy} = \left( \frac{C_{DA}}{m} \right) \frac{q\rho}{\sin \gamma} - \rho g - \beta q \quad (34)$$

and

$$\begin{aligned} \frac{1}{q} \frac{dq}{ds} &= -\sin \gamma \frac{1}{q} \frac{dq}{dy} \\ &= -\sin \gamma \left[ \left( \frac{C_{DA}}{m} \right) \frac{\rho}{\sin \gamma} - \frac{2g}{v^2} - \beta \right] \end{aligned} \quad (35)$$

Inserting equation (35) and also the definition of  $P_1(s)$  (eq. (9)) in equation (29), we get finally as a general criterion to be fulfilled by the dynamic stability parameter  $K$

$$K < -1 + \left( \frac{W}{C_{DA}} \right) (\sin \gamma) \left[ \frac{1}{q} + \frac{\beta}{g\rho} + \frac{1}{g\rho \sin \gamma} \frac{C_{m\alpha}'(s)}{C_{m\alpha}(s)} \right] \quad (36)$$

where

$$K = \frac{1}{C_D} \left[ -C_{L\alpha} + \left( \frac{l}{\sigma} \right)^2 (C_{mq} + C_{m\dot{\alpha}}) \right]$$

Approximate criterion.— The derivation leading to equation (36) has not required the introduction of approximations either to the trajectory equations or to the aerodynamic coefficients. When equation (27) is used to represent the oscillation amplitude rather than equation (28), however, it is advisable to use a convergence criterion that is consistent with the approximations introduced in the derivation of equation (27). With the approximations indicated by equations (23) in force and with constant aerodynamic coefficients the convergence criterion obtained from differentiation of equation (27) takes the form

$$-\frac{K}{2} \frac{u'(s)}{u(s)} - \frac{1}{4} \frac{q'(s)}{q(s)} < 0 \quad (37)$$

Under the conditions defined by equations (23), the derivatives indicated in equation (37) can be evaluated from the static trajectory equations

used by Chapman in reference 3. (The term  $u'(s)/u(s)$  is already available as equation (25).) The convergence criterion becomes

$$K < -1 - \frac{L}{D} \frac{\sin 2\gamma}{2} + \left( \frac{W}{C_D A} \right) (\sin \gamma) \left[ \frac{\beta}{g\rho} + \frac{1}{q} (1 - \bar{u}^2) \right] \quad (38)$$

Oddly enough, it turns out that the more precise expression, equation (36), is also simpler in form. However, so long as the conditions imposed by equations (23) are satisfied, the differences between results computed from equations (38) and (36) should be insignificant.<sup>1</sup>

To summarize, it is advised that equations (28), (29), and (36) be used when the properties of the trajectory are known precisely. The results (27), (37), and (38) are those appropriate for use with constant aerodynamic coefficients and in conjunction with trajectories computed from Chapman's approximate analysis (ref. 3).

## DISCUSSION

Let us now apply the results just developed to a study of the oscillatory behavior of vehicles whose decelerations during their descent through the atmosphere appear to be within the bounds of human tolerance. We have chosen as examples a series of nonlifting and lifting vehicles with values of entrance angle ranging from  $0^\circ$  to  $4^\circ$  and drag-loading parameter,  $W/C_D A$ , of 10, 30, and 100 pounds per square foot. For these examples the static flight trajectories were computed by the method of reference 3 with the following conditions common to all cases:

(a) Constant aerodynamic coefficients

$$(b) \bar{v}_i = \frac{v_i}{\sqrt{gr}} = 1$$

$$(c) y_i = 400,000 \text{ ft}$$

$$(d) \rho = \rho_0 e^{-\beta y}$$

with

---

<sup>1</sup>Note that the spurious  $L/D$  term in equation (38) may be discarded in comparison with the first term, since by virtue of the second of equations (23) we have

---


$$\left| \frac{L}{D} \frac{\sin 2\gamma}{2} \right| \leq \left| \frac{L}{D} \tan \gamma \right| \ll 1$$


---

$$\rho_0 = 0.0027 \text{ slugs/ft}^3$$

$$\beta = \frac{1}{23,500} \text{ ft}^{-1}$$

The choice  $\bar{V}_i = 1$  implies that the trajectories are those corresponding to entry from circular satellite orbit, with the altitude at entry being in the neighborhood of 80 miles (condition c).

### Nonlifting Vehicles

Figure 1 shows the deceleration history in g's for nonlifting vehicles having initial flight-path angles of  $0^\circ$ ,  $2^\circ$ , and  $4^\circ$ . For all but a portion of the  $4^\circ$  case, the decelerations are seen to be below the level of 11.5 g considered to be an upper bound of human tolerance in reference 3. Hence, for the chosen set of initial conditions, the entry angle range  $0^\circ$  to  $4^\circ$  appears to cover the spectrum of usable trajectories for manned nonlifting vehicles. The case  $\gamma_i = 22^\circ$  is included in figure 1 to illustrate the magnitude of decelerations typical of trajectories having steeper entry angles, such as are experienced by long-range ballistic missiles. This case will again be used in subsequent figures as illustrative of ballistic missile trajectories, in order to compare the oscillatory behavior of manned vehicles with that typical of ballistic missiles.

Effect of K.— The effect of the dynamic stability parameter, K, on the oscillatory motion can be demonstrated by use of the convergence criterion, equation (38). Since the sign of the expression determines whether a vehicle's oscillations are convergent or divergent, setting the expression equal to zero gives the set of circumstances signifying a changeover from convergent to divergent oscillations or vice-versa. Then, at each point on the known trajectory, one can solve for the value of K that makes the expression zero. The locus of such values of K plotted against altitude therefore forms a boundary which separates the range of altitudes over which oscillatory divergence is possible from the range over which it is not. Such boundary curves are shown in figure 2 for the three cases ( $\gamma_i = 0^\circ$ ,  $2^\circ$ ,  $4^\circ$ ) considered suitable for manned vehicles and also for the ballistic missile case,  $\gamma_i = 22^\circ$ . The drag-loading parameter  $W/C_D A$  is 30 pounds per square foot.<sup>2</sup>

The significance of the figure is as follows: Vehicles whose values of K and altitude fall within the boundaries of their respective curves

---

<sup>2</sup>The assumption of constant aerodynamic coefficients is undoubtedly invalid at subsonic and transonic speeds. For this reason the curves are terminated below an altitude corresponding to sonic flight speed ( $\bar{V} \approx 0.04$ ). It would be possible to continue the curves if the variations with Mach number of the aerodynamic coefficients were given; one would use equation (36) rather than (38) in this case.

---



will experience divergent oscillations over the altitude range within the boundaries. Thus, for example, the curve for the ballistic missile ( $\gamma_1 = 22^\circ$ ) indicates that a missile whose value of  $K$  is  $-0.4$  will experience divergent oscillations during its descent through the altitude range from 110,000 feet to 72,000 feet. On the other hand, for a missile with  $K = +0.4$ , the oscillations begin to diverge at 130,000 feet and continue to diverge thereafter.

The main point that becomes evident from figure 2 is that the consequences of a deficiency of aerodynamic damping ( $K > 0$ ) can be more serious for manned vehicles than they are for ballistic missiles. This follows from the observation that for the same value of positive  $K$  the amplitude of oscillation of the manned vehicle begins to diverge at a higher altitude, so that by the time the amplitude of the ballistic missile also begins to diverge the manned vehicle has already sustained a divergent oscillation over an altitude span of some 30,000 to 55,000 feet. The reason for this becomes clear from inspection of the case  $K = 0$ , corresponding to zero aerodynamic damping. Referring to equation (37), we see that divergence begins in this case when  $q'(s) = 0$ ; that is, at the altitude where dynamic pressure is a maximum. Hence, any factor (smaller entrance angle being one) which tends to raise the altitude at which  $q$  is maximum will also tend to increase the seriousness of the dynamic stability problem for cases where  $K \geq 0$ .

Amplitude ratios.- The value of a plot such as figure 2 is that one can determine immediately whether or not the possibility exists of a dynamic stability problem for a vehicle with a given value of  $K$ . If a problem is indicated, however, its severity is still in doubt, since the amplitude ratio may be so small when divergence begins, or divergence may occur at so low an altitude, that the amplitude cannot grow to serious magnitudes in the time remaining before the vehicle lands. To investigate the severity of the problem, the actual amplitude history is required.

Amplitude ratios have been evaluated from equation (27) for values of  $K$  of  $-2$ ,  $0$ , and  $+2$ , representative of vehicles with a large amount of aerodynamic damping, zero aerodynamic damping, and a large deficiency of aerodynamic damping, respectively. These are plotted as functions of altitude for a habitable vehicle ( $\gamma_1 = 0^\circ$ ) in figure 3(a) and for a ballistic missile ( $\gamma_1 = 22^\circ$ ) in figure 3(b). The drag-loading parameter is again 30 lb/sq ft in both cases. In addition, the dimensionless velocity  $\bar{V}$  is shown.

The results show that with  $K = -2$  the amplitude ratio diminishes very rapidly for both vehicles. For zero aerodynamic damping ( $K = 0$ ), the motion is divergent below the altitude for maximum  $q$ , but the amplitude does not grow excessively for either the manned or ballistic vehicle before sonic velocity is reached. For  $K = +2$ , however, it is clear that a deficiency of aerodynamic damping of this magnitude leads to a divergent oscillation that may be of serious consequence. In this case the fact that divergence begins at a higher altitude for the manned

vehicle than it does for the ballistic missile makes the dynamic stability problem for the former vehicle considerably more severe. Thus, the amplitude ratio for the manned vehicle has already reached 1 at an altitude of 115,000 feet (fig. 3(a)) whereas the amplitude ratio of the ballistic missile at this altitude is still only 0.13 (fig. 3(b)).

Effect of  $\gamma_i$  and  $W/C_D A$ . - Having determined that the possibility of a serious dynamic stability problem exists only for positive values of  $K$ , we shall confine the remainder of the discussion to this case, letting  $K = +2$ .

Figure 4 shows the effect on amplitude ratio of varying the initial flight-path angle  $\gamma_i$  for one value of  $W/C_D A$ , whereas figure 5 shows the effect of varying  $W/C_D A$  for one value of  $\gamma_i$ . It will be seen that increasing either  $\gamma_i$  or  $W/C_D A$  tends to diminish the severity of the dynamic stability problem for manned vehicles, although the former effect is small because of the small range of entry angles available for feasible manned flight trajectories. Both of these effects are simply manifestations of the single fact already pointed out, that factors tending to lower the altitude at which  $q$  is maximum also tend to diminish the severity of the dynamic stability problem.

One final point should be made regarding the effects of  $\gamma_i$  and  $W/C_D A$  on the oscillatory behavior of ballistic missiles and manned vehicles. To isolate the effect of entry angle in figure 4 the two vehicles were given the same value of  $W/C_D A$ , namely, 30 lb/sq ft. We recognize that while this is a reasonable figure for the manned vehicle, the drag-loading parameter of a ballistic missile will generally be considerably larger. Hence, in general, the ballistic missile will benefit from larger values of both  $\gamma_i$  and  $W/C_D A$ . Thus, in figure 5 even the curve for the manned vehicle with the highest value of  $W/C_D A$ , 100 lb/sq ft, would fall above and to the right of a typical ballistic-missile curve. It is the combination of beneficial factors, larger  $\gamma_i$  and larger  $W/C_D A$ , that leads one to the conclusion that for a ballistic missile, dynamic instability is a potential source of difficulty only in its terminal phase of flight. In contrast, it is seen that dynamic instability is a source of difficulty for the manned vehicle over a significant portion of its trajectory. We should note, however, that a compensating factor also exists for the manned vehicle that may ease the problem of controlling oscillatory divergence: The maximum value of dynamic pressure experienced by manned vehicles will be very much less than that of ballistic missiles. Hence, although control of the oscillatory divergence of the manned vehicle may be more urgently required, the frequencies at which the controlling device must operate, being proportional to  $\sqrt{q}$ , will be very much smaller for the manned vehicle than they are for the ballistic missile.

## Lifting Vehicles

To study the effect of lift, we have chosen a vehicle having a lift-to-drag ratio of 0.5 and a drag-loading parameter of 30 lb/sq ft. The range of initial flight-path angles is  $0^\circ$  to  $4^\circ$ , as for the nonlifting vehicles. The degree to which even this small amount of lift is effective in reducing decelerations may be illustrated by noting that the maximum deceleration experienced by the lifting vehicle in the worst case ( $\gamma_i = 4^\circ$ ) is only 3.6 g as compared to 13.3 g for the nonlifting vehicle with  $\gamma_i = 4^\circ$ . Hence we are assured that at least from the standpoint of tolerable decelerations the vehicle under consideration is habitable.

Effect of K.- A comparison of the convergence boundary curve for the lifting vehicle with the curve for the nonlifting vehicle is shown in figure 6 for one entrance angle,  $\gamma_i = 0^\circ$ . The figure shows that for vehicles deficient in aerodynamic damping ( $K > 0$ ) the use of lift increases the severity of the dynamic stability problem in about the same proportion as it was increased by the use of small initial flight-path angles for nonlifting vehicles (fig. 2). Consideration of the  $K = 0$  case reveals that this is once again attributable to the fact that the altitude at which  $q$  is a maximum has been raised still further.

Amplitude ratios.- Amplitude ratios for the lifting vehicle with  $\gamma_i = 0^\circ$  and  $K = -2, 0, +2$  are shown in figure 7. These are to be compared with the results for the equivalent nonlifting vehicle given in figure 3(a). It is noted that for  $K = 0$  (and presumably for a range of small  $K$ ) the amplitude history for the lifting vehicle is not significantly worse than that for the nonlifting vehicle. For  $K$  as large as +2, however, it will be noted that the divergence is considerably more severe.

Amplitude ratio and velocity histories for the lifting vehicle with initial flight-path angles of  $2^\circ$  and  $4^\circ$  are shown in figures 8(a) and 8(b), respectively. For initial angles other than  $0^\circ$ , the trajectory of the lifting vehicle differs from that of the nonlifting vehicle in that the lifting vehicle makes small skips as the lift force momentarily overcomes gravity. The strange behavior of the amplitude ratio curves simply reflects the behavior of the static flight trajectory. Thus as the vehicle first gains and then loses altitude, the concurrent changes in dynamic pressure cause the motion first to diverge and then to converge. Finally, when the velocity has slowed sufficiently, the oscillatory amplitude behavior is almost identical to that for  $\gamma_i = 0^\circ$  (fig. 7).

## CONCLUDING REMARKS

An analysis has been carried out of the oscillatory motions developed by vehicles as they traverse arbitrarily prescribed trajectories through

the atmosphere. Expressions were derived that describe the oscillatory motions and, in particular, the envelope of oscillations, as continuous functions of the properties of the trajectory. For the special case of constant aerodynamic coefficients the envelope of oscillations has the simple form

$$\alpha_{\max} = \frac{Cu^{-K/2}}{q^{1/4}}$$

where  $q$  and  $u$  are, respectively, the dynamic pressure and horizontal component of velocity,  $K$  is a measure of the aerodynamic damping properties of the vehicle, and  $C$  is an arbitrary constant.

Results of the analysis were used to study the oscillatory behavior of vehicles which have deceleration histories that remain within bounds of human tolerance. It was determined that for vehicles deficient in aerodynamic damping ( $K > 0$ ), the factor governing the seriousness of the divergent oscillations which occur is the altitude at which dynamic pressure is a maximum. The decelerations of manned vehicles are maintained within tolerable limits by the use of small initial flight-path angles or by the use of lift. Since both tend to raise the altitude at which dynamic pressure is maximum, it was concluded that the dynamic stability problem of manned nonlifting vehicles deficient in aerodynamic damping may be more severe than that of comparable ballistic missiles, and that the use of lift further increases the severity of the problem. On the other hand, it is recognized that a compensating factor exists in that the maximum value of  $q$  experienced by manned vehicles will be very much smaller than that of ballistic missiles. This factor may serve to ease the problem of controlling the oscillatory divergence of manned vehicles, since the frequencies at which a control must operate, being proportional to  $\sqrt{q}$ , will be very much lower for manned vehicles than they are for ballistic missiles.

Ames Research Center  
National Aeronautics and Space Administration  
Moffett Field, Calif., Dec. 2, 1958

#### REFERENCES

1. Friedrich, Hans R., and Dore, Frank J.: The Dynamic Motion of a Missile Descending Through the Atmosphere. Jour. Aero. Sci., vol. 22, no. 9, Sept. 1955, pp. 628-632, 638.
2. Allen, H. Julian: Motion of a Ballistic Missile Angularly Misaligned With the Flight Path Upon Entering the Atmosphere and Its Effect Upon Aerodynamic Heating, Aerodynamic Loads, and Miss Distance. NACA TN 4048, 1957.

3. Chapman, Dean R.: An Approximate Analytical Method for Studying Entry Into Planetary Atmospheres. NACA TN 4276, 1958.
4. Tobak, Murray, and Allen, H. Julian: Dynamic Stability of Vehicles Traversing Ascending or Descending Paths Through the Atmosphere. NACA TN 4275, 1958.
5. Wintner, Aurel: The Schwarzian Derivative and the Approximation Method of Brillouin. Quart. Appl. Math., vol. XVI, no. 1, April 1958, pp. 82-86.



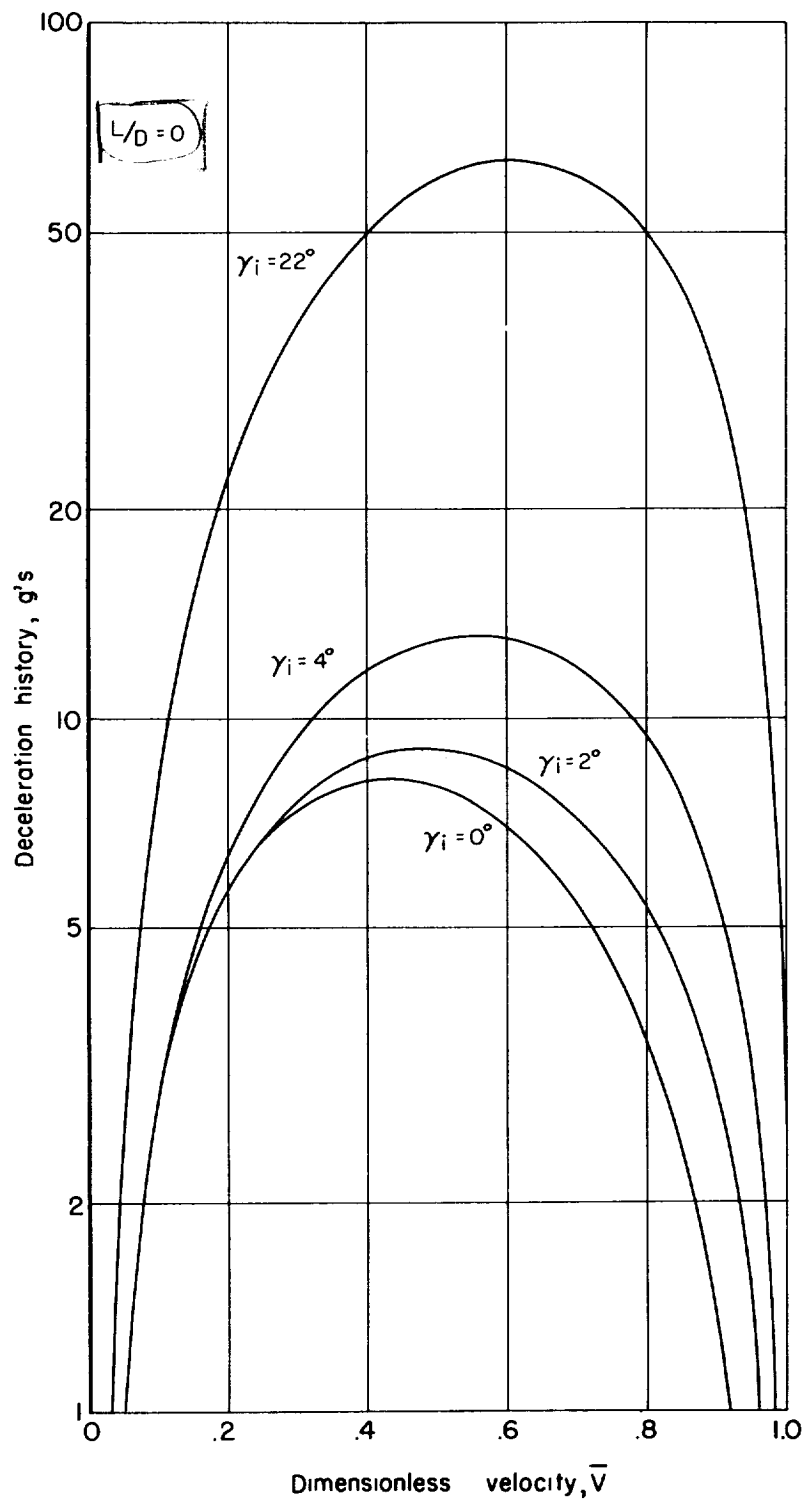


Figure 1.- Deceleration histories for nonlifting vehicles.

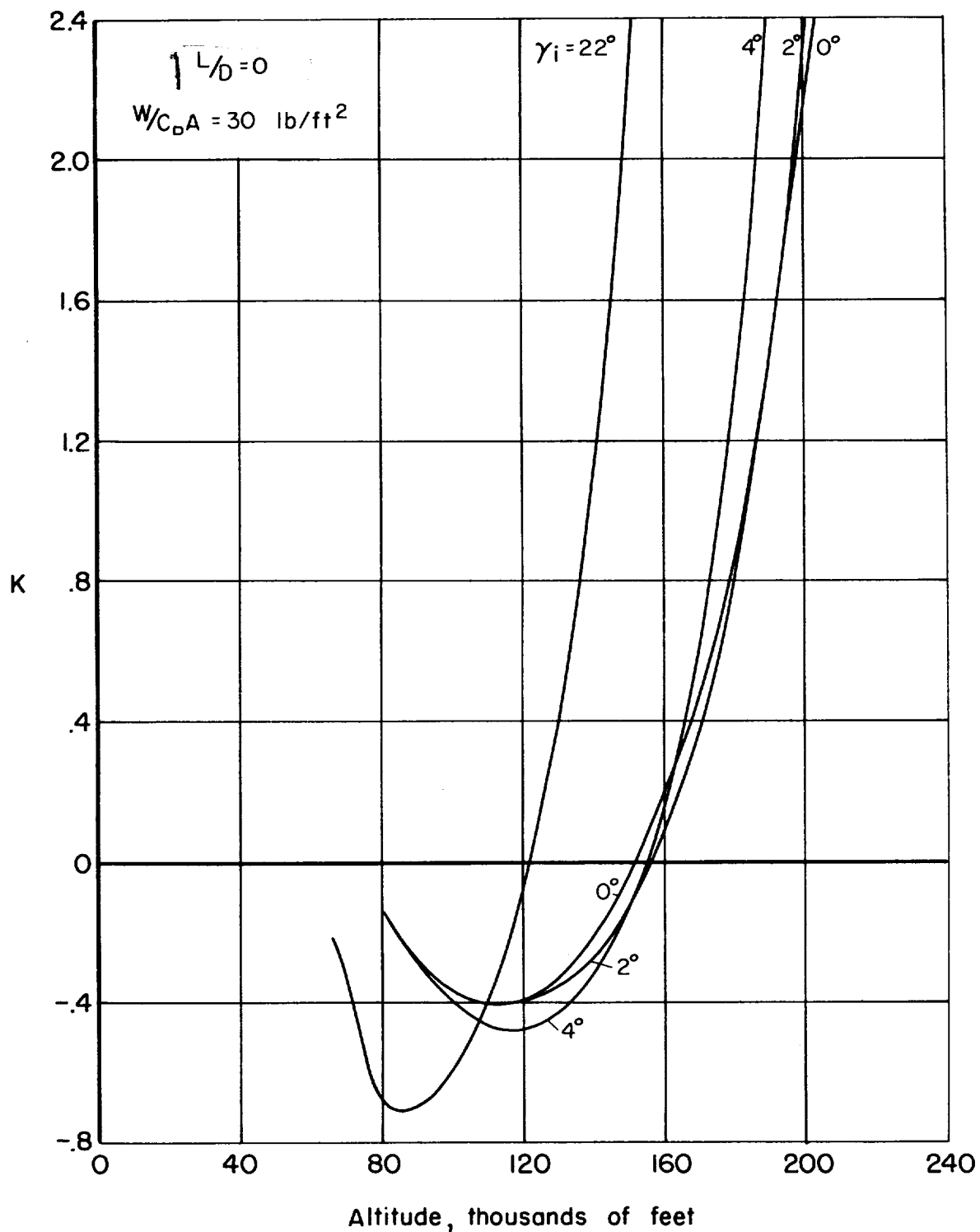
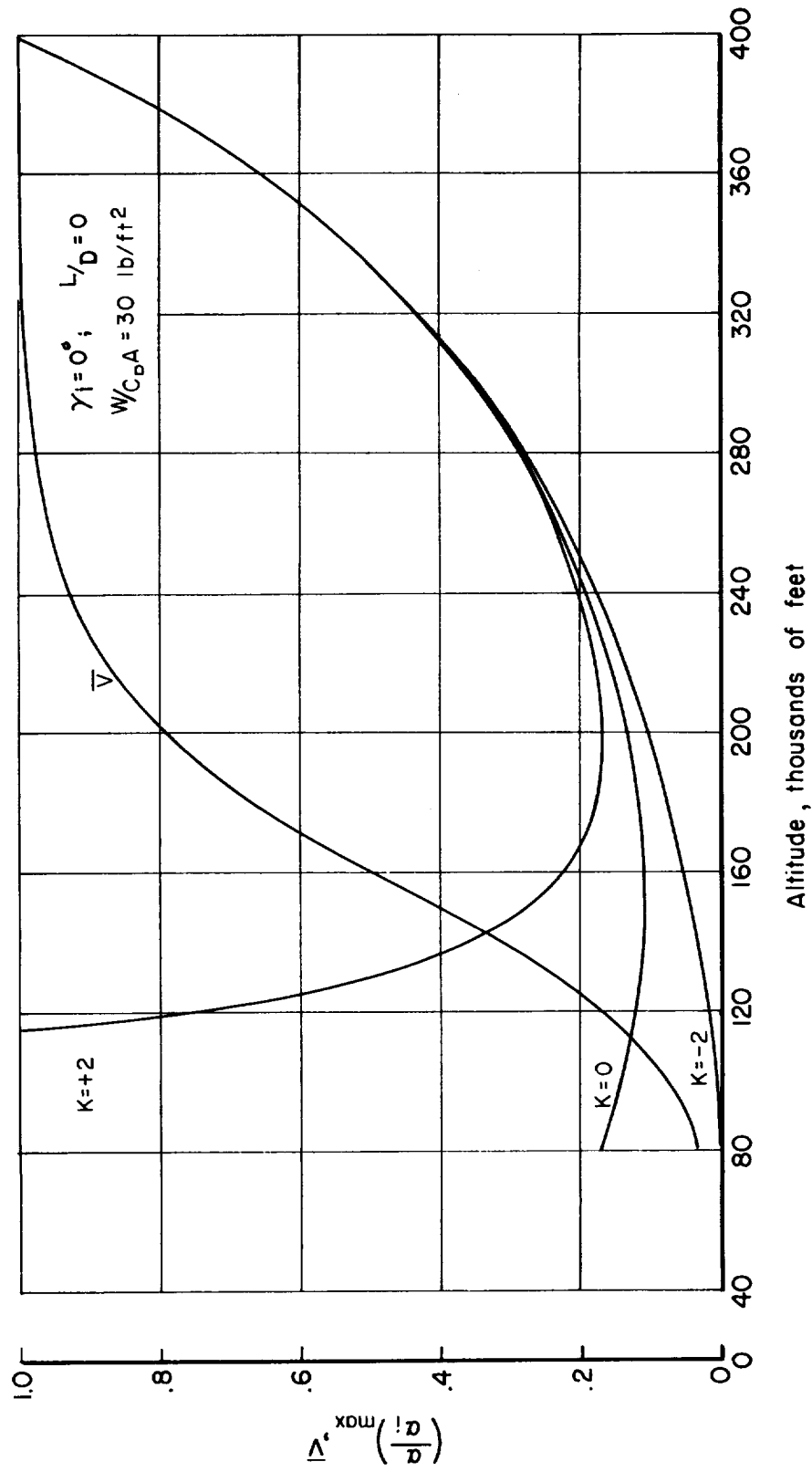


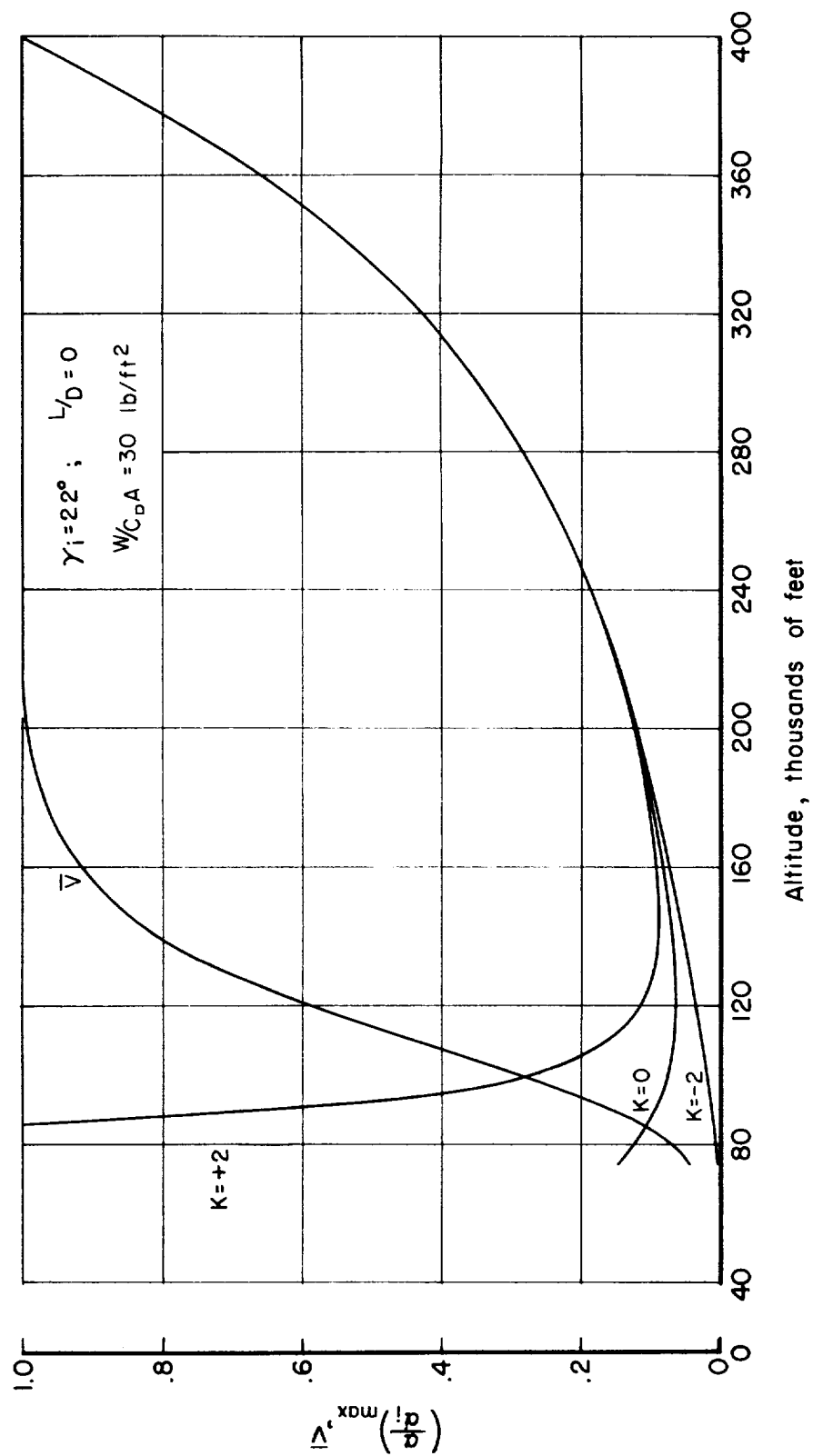
Figure 2.- Convergence-boundary curves for nonlifting vehicles.





(a)  $\gamma_i = 0^\circ$

Figure 3.- Oscillation-amplitude histories for nonlifting vehicles.



(b)  $\gamma_i = 22^\circ$

Figure 3.- Concluded.

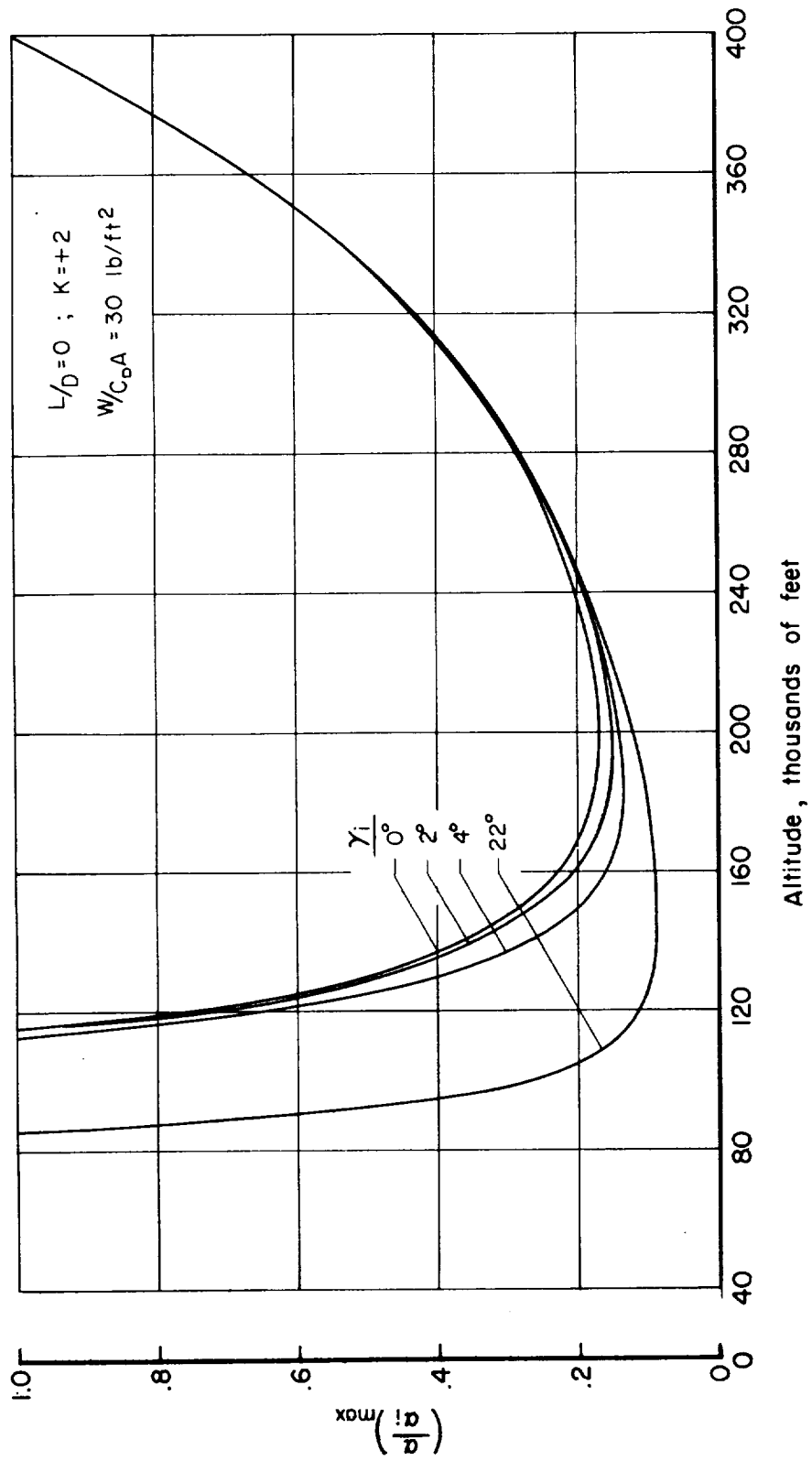


Figure 4.- Effect of initial flight-path angle on oscillation amplitudes for nonlifting vehicles.

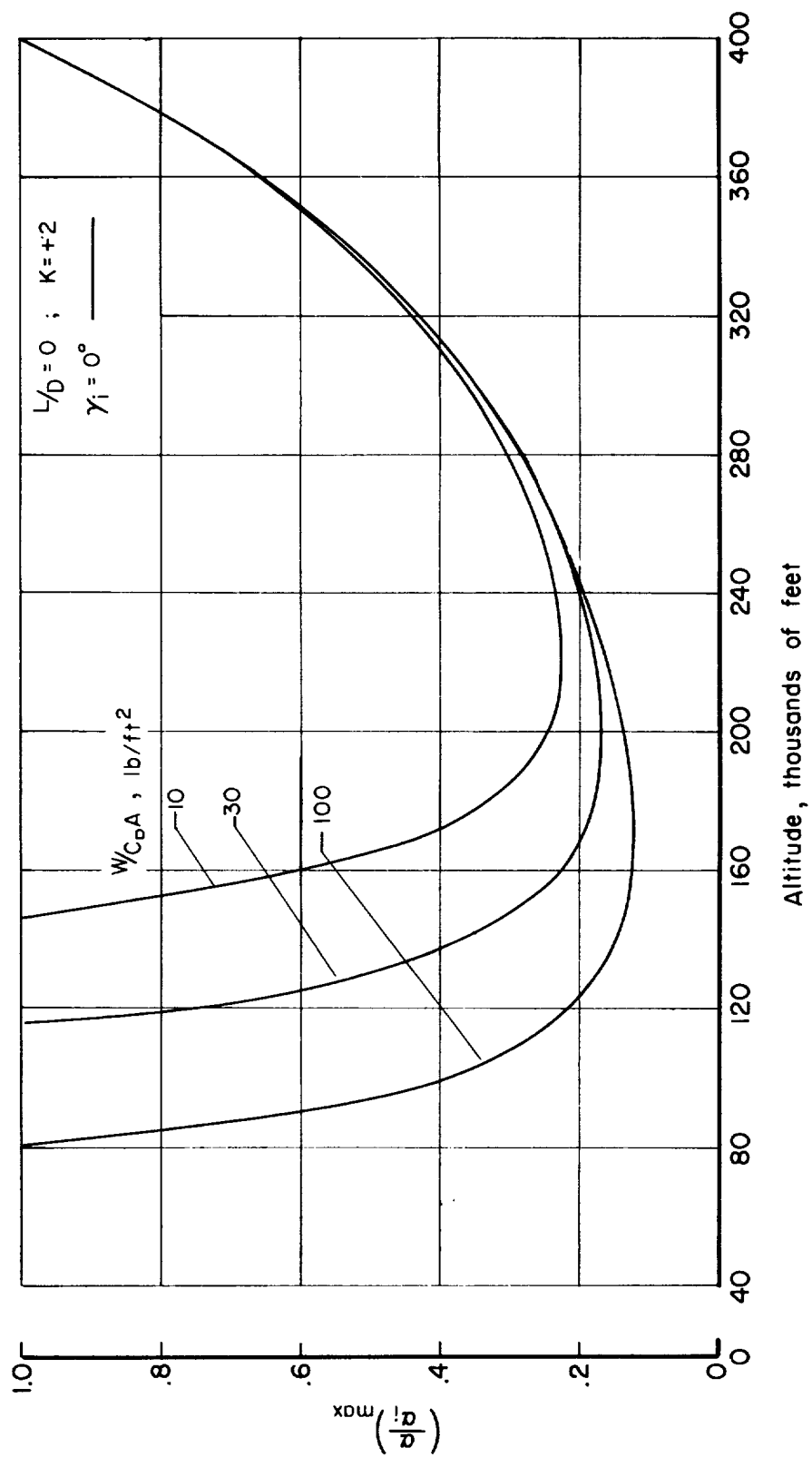


Figure 5.- Effect of drag-loading parameter on oscillation amplitudes for nonlifting vehicles.

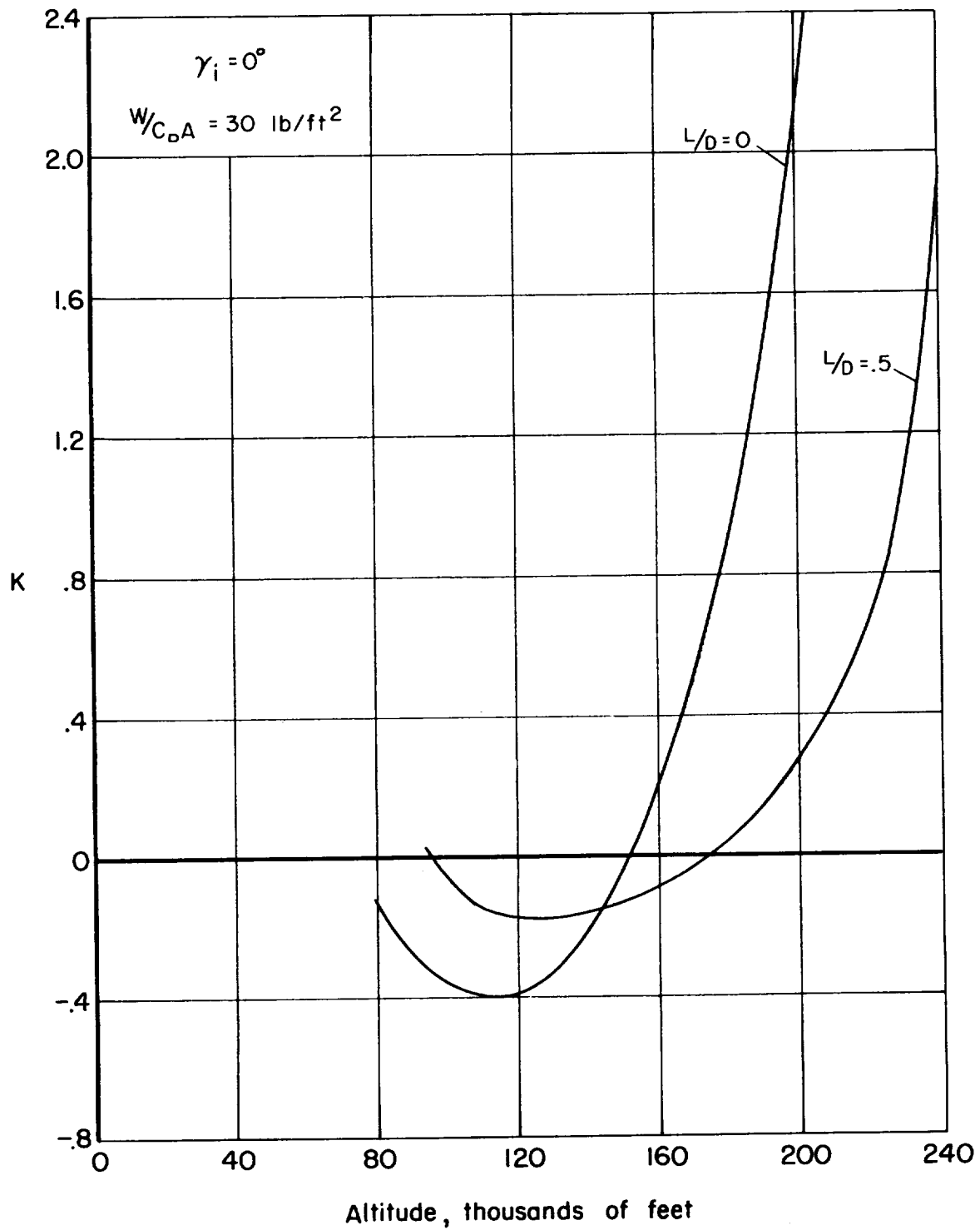


Figure 6.- Comparison of convergence-boundary curves for lifting and nonlifting vehicles with zero initial flight-path angles.

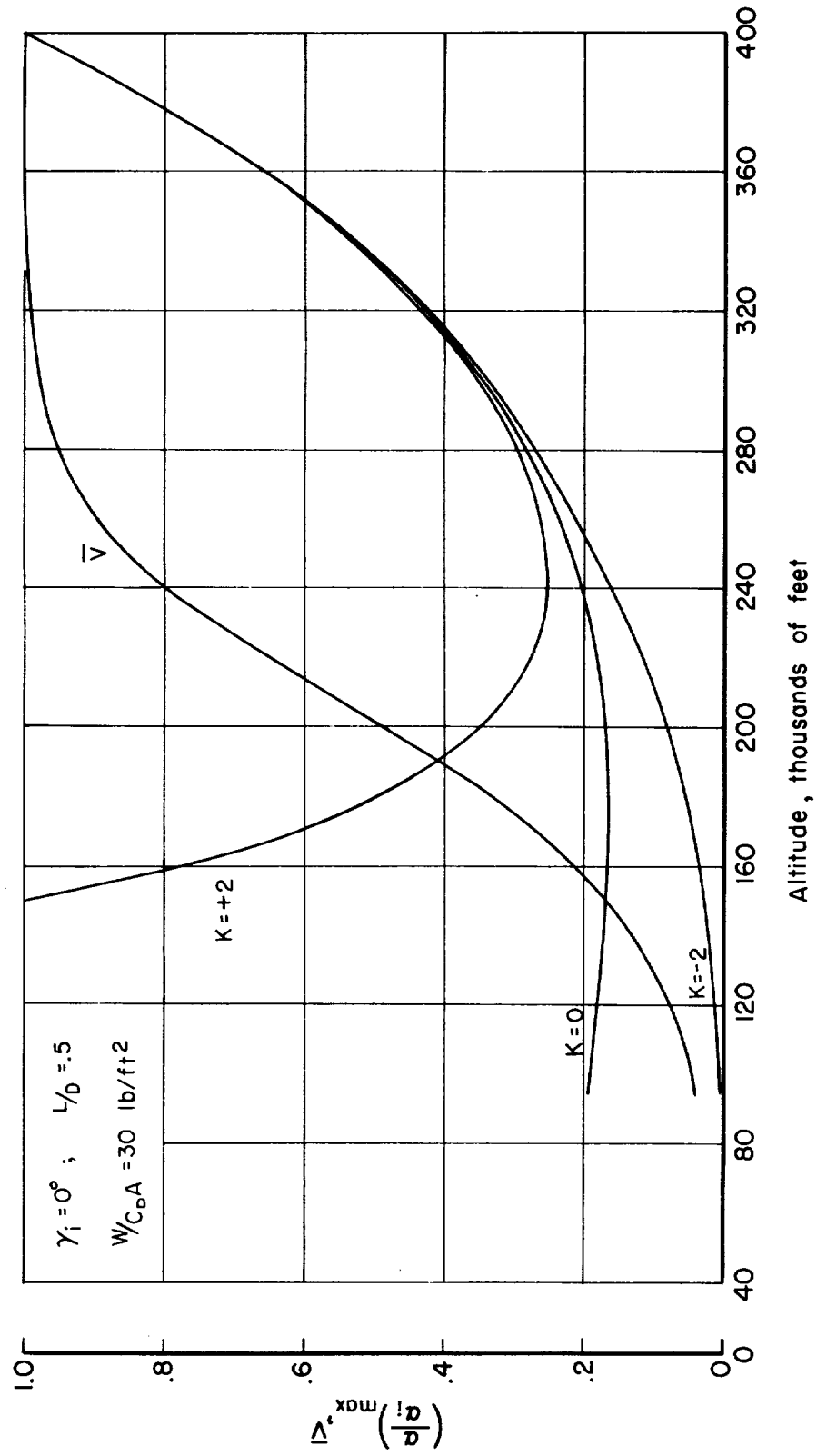
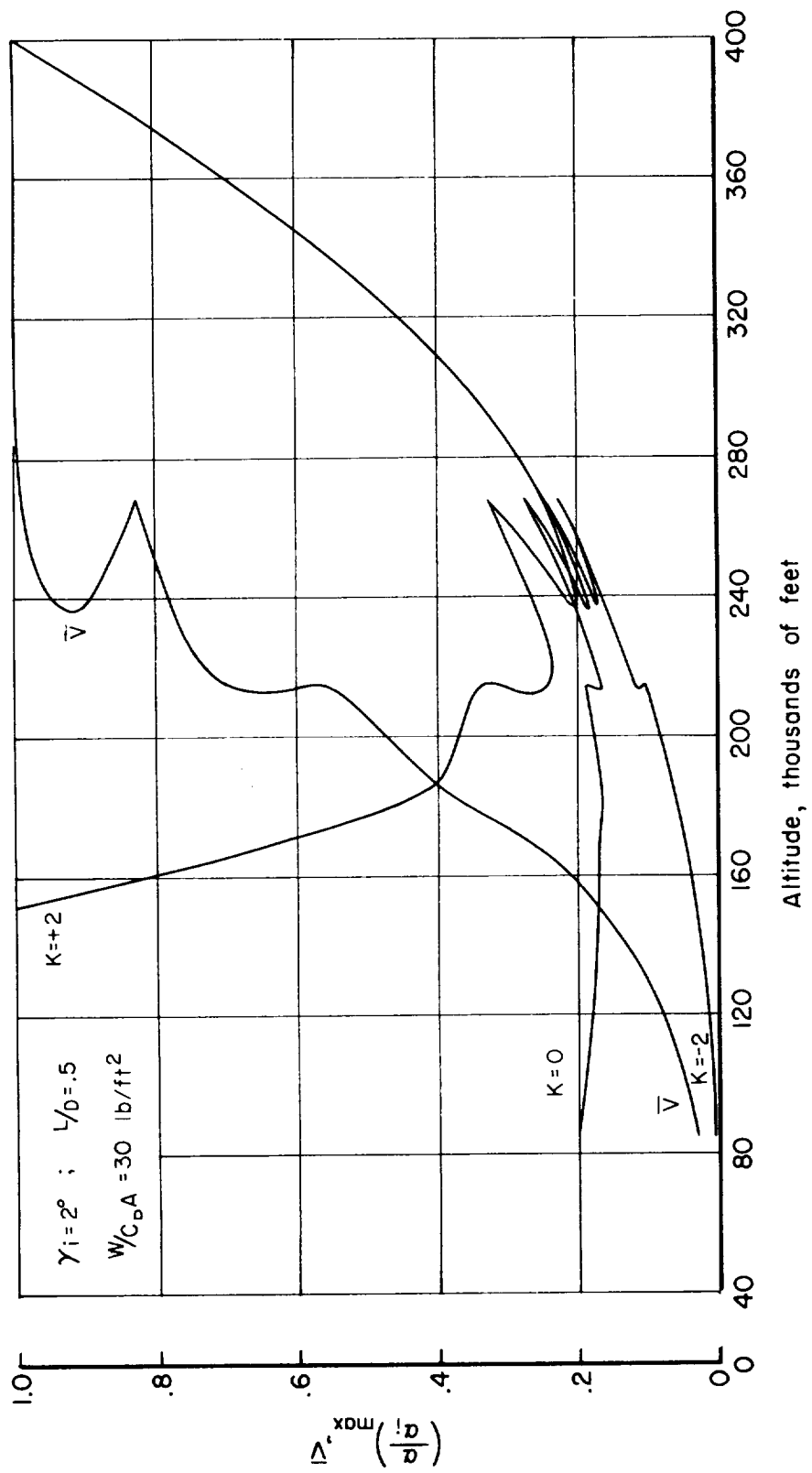
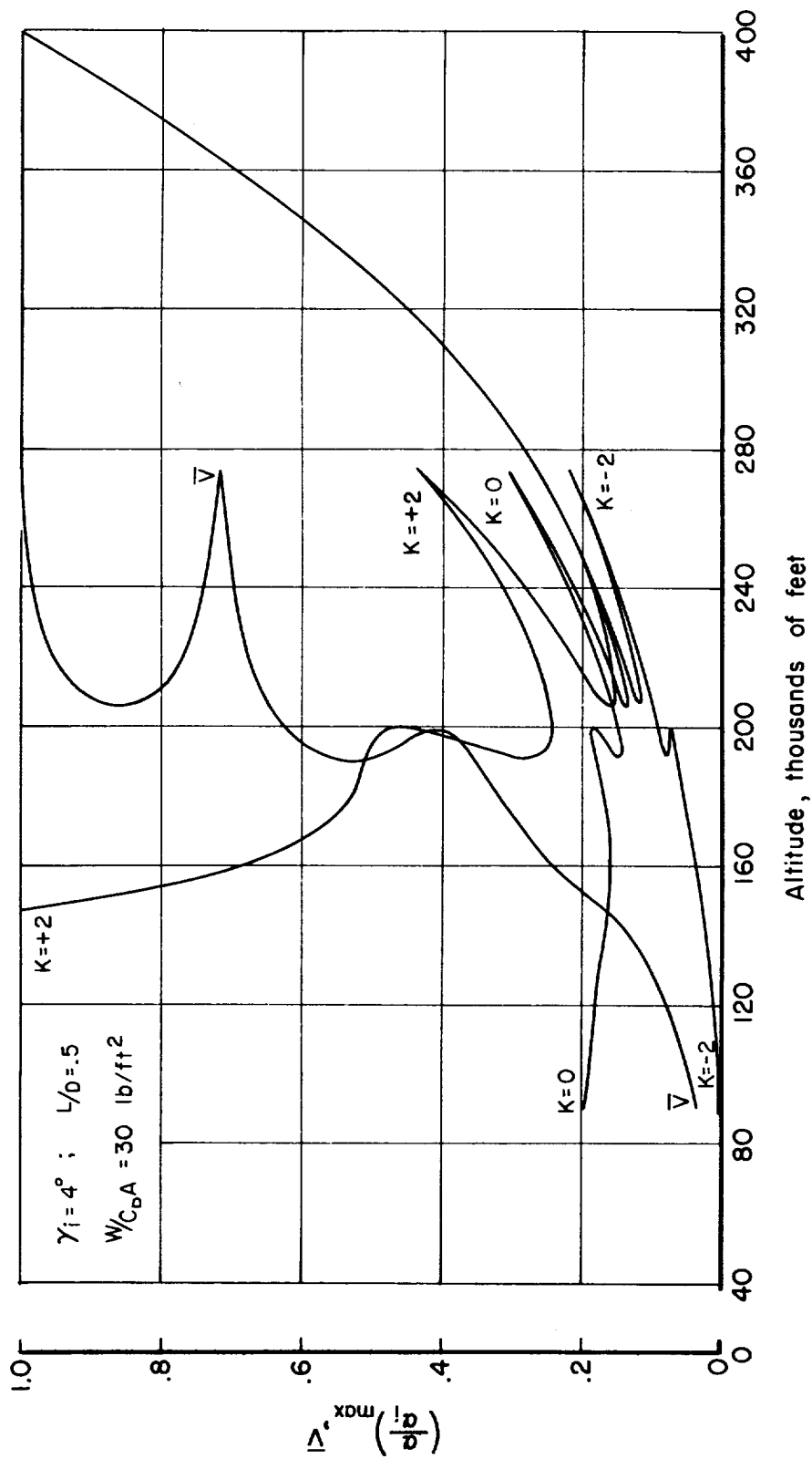


Figure 7.- Oscillation-amplitude histories for lifting vehicles with zero initial flight-path angle.



(a)  $\gamma_i = 2^\circ$

Figure 8.- Oscillation-amplitude histories for lifting vehicles.



(b)  $\gamma_i = 4^\circ$

Figure 8.- Concluded.